Proceedings of the 2022 IEEE
International Conference on Robotics and Biomimetics
December 5-9, 2022, Xishuangbanna, China

Design and Preliminary Evaluation of a Lightweight, Cable-Driven Hip Exoskeleton for Walking Assistance*

Wei Jin and Hongbin Fang

Abstract—**The hip exoskeleton has demonstrated the capability of enhancing human locomotion performance during walking. However, few of them reached the ideal effect and went out of the lab due to excessive weight, lack of degree of freedom and user discomfort. In this paper, we present a cable-driven hip exoskeleton that concentrates on lightweight, comfortability and human-machine interaction. The total weight of the device is 3.15 kg excluding the real-time controller. Active cable-driven actuators and passive actuators based on torsional springs are developed to provide assistive force in the sagittal plane, and allow the hip to move freely in the coronal plane. We proposed a hierarchical controller that calculates the motor current command based on sensory information and user instruction, and validated the usability and effectiveness of the exoskeleton through a series of evaluation experiments. The results showed the exoskeleton can provide 14% of energy supply per step on average during walking. Our work may provide a possible solution for the future lightweight, high-performance, and humanized hip exoskeleton.**

I. Introduction

In the past 20 years, robotic exoskeletons have demonstrated the capability to assist both people with gait disorders and ones who walk normally. An exoskeleton is a wearable robot that can provide support, assistance, or protection through interaction with human limbs, and can be a promising way of reducing muscle fatigue, metabolic expenditure, or injury rates during walking [1]. Since the first practical lower limb exoskeleton *BLEEX* for loaded walking was created and reported to the world [2-3], the study of exoskeleton has never waned. Various commercial lower-limb exoskeletons, such as ReWalk [4], Ekso [5], HAL [6], and Indego [7], had also achieved elementary success meanwhile.

Biological studies have shown that the hip joint requires more energy expenditure than the ankle joint and the knee joint do when generating a similar amount of mechanical joint power [8]. It gives a more promising optimization space for energy cost reduction during walking. Moreover, the hip joint's better endurance of large external torque or force allows more possibilities for assistance strategies to be implemented. Honda developed a hip exoskeleton that assists users in adopting a more efficient posture, muscle usage and walking ratio [9]. Two direct current (DC) motors were placed on both sides of the hip joints as actuators to provide hip flexion and extension torques. Zhang et al. developed a 4-DoFs hip exoskeleton named *NREL-Exo*, capable of assisting in both sagittal and frontal planes during walking [10]. The device with four DC motors actuating four serial elastic actuators (SEAs) weighed 9.2 kg excluding the power source. Giovacchini et al. developed a hip exoskeleton named *APO*, endowed with two SEAs for hip flexion-extension assistance [11]. It weighed 4.2 kg excluding the on-board control unit. However, the actuators on both sides of the hip joints are so thick that the user's hand movements were affected during walking. Asbeck et al. developed a fully portable hip exosuit that assisted in the sagittal plane through a seatbelt driven by a motor placed on the backpack frame [12]. The exosuit, weighing 10.7 kg in total, was designed to generate 30% of the nominal biological torques for walking.

As mentioned above, most hip exoskeletons implement direct flexion/extension torque for assistance. This strategy is direct but requires the actuator (DC motor mostly) to be placed beside the hip joint, which may lead to interference with the user's hand movements because of the unavoidable protuberance of the motors from the sides of the exoskeleton. In addition, since the torque is directly applied to the hip joint, discomfort and even injury may occur once the assistance is inappropriate or good alignment is not ensured. One of the resolutions is to provide assistive force through a cable or belt, in which case the actuator can be placed elsewhere to avoid the problems above. Chiu et al. developed an assistive hip exoskeleton, utilizing Bowden cables to transmit mechanical power from the on-board motors [13]. This rigid-flexible hybrid characteristic of the actuation allows wider movement space and stronger assistance for the user.

Furthermore, three principles should be abided by for a user-friendly exoskeleton design: comfortability, interactivity, and portability, which also make up the current challenges of hip exoskeletons. Comfortability requires the exoskeleton to be lightweight and adaptable to users of various shapes and sizes, and interference with natural motions should be avoided as far as possible. Interactivity requires the adaptability of the exoskeleton to user commands through motion, voice, button or interface. Portability means as few on-board components of the exoskeleton as possible, and that the endurance of the battery should be taken into consideration.

The goal and main contribution of this study is to develop an assistive hip exoskeleton based on the three principles above. A lightweight, multi-degree-of-freedom cable-driven hip exoskeleton with both active and passive actuators is presented, allowing assistance in the sagittal plane and free movement of the hip joint in the coronal plane. Multiple adjustments are supported for comfortability and customization. We then proposed a hierarchical adaptive control framework that allowed the exoskeleton to switch

*This research was supported by the Shanghai Rising-Star Program under Grant No.20QA1400800. (Corresponding author: Hongbin Fang.)

The authors are with the Institute of AI and Robotics, Fudan University, Shanghai 200433, China. They are also with the MOE Engineering Research Center of AI & Robotics and Shanghai Engineering Research Center of AI & Robotics, Fudan University, Shanghai 200433, China (email: wjin21@m.fudan.edu.cn; fanghongbin@fudan.edu.cn;).

2022 IEEE International Conference on Robotics and Biomimetics (ROBIO) | 978-1-6654-8109-0/22/$31.00 ©2022 IEEE | DOI: 10.1109/ROBIO55434.2022.10011746

between *FOLLOW* and *ASSIST* modes. Preliminary evaluation experiments were performed to validate the usability and effectiveness of the exoskeleton. Finally, the paper will end with a discussion and a brief conclusion.

II. Mechanical Design

The mechanical design of the unilateral assistive hip exoskeleton, as shown in Fig. 1(a), is based on the consideration of the three principles mentioned above. The subject wearing the hip exoskeleton is shown in Fig. 1(b). The proposed device consists of three segments: waist segment, hip segment and thigh segment. The overall weight of the exoskeleton, including the battery, is 3.15 kg.

A. Waist Segment

For the waist segment, a lightweight, portable battery (TB48S, DJI, Shenzhen, China) and a motor driver (C620, DJI, Shenzhen, China) are mounted on the right side of the waist brace, which can be attached to the waist of the person by velcro. A base, made of carbon fiber and particularly designed for motor position adjustment, is installed on the back of the waist brace. A portable motor (M3508, DJI, Shenzhen, China) is fixed on a carbon fiber base. The cable functions to transmit force from the motor to the thigh, with its ends fixed to the motor output shaft and the ring of the force sensor installed on the thigh brace, respectively.

The adjustable carbon fiber base, shown in Fig. 2, is composed of two fixed plates and two moving plates. The two moving plates, lying in the same sagittal plane, are sandwiched between the two fixed plates. The cable holder allows the cable to pass through it and functions as a fixed pulley as well as a cable-motion-confinement element. The moving plates can slide along the groove so that the plane formed by the output shaft, cable holder, and force sensor is parallel to the sagittal plane of the human body. This simple but useful design can avoid disturbing forces in unexpected directions effectively when the exoskeleton assists with walking. The adjustable range of the width of the base is 280 mm ~ 340 mm, which can satisfy the requirements of the vast majority.

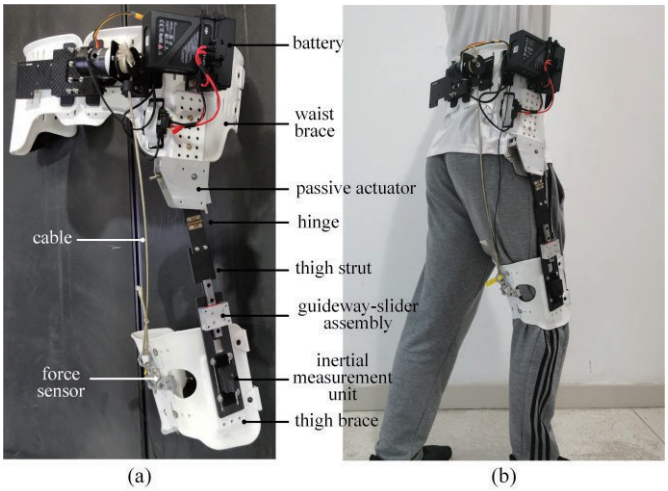

Fig. 1. The prototype of the hip exoskeleton. (a) Prototype. (b) Man wearing the prototype.

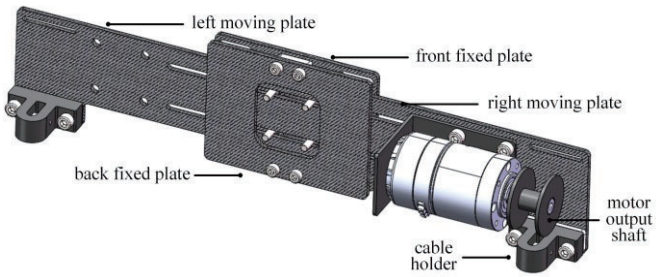

Fig. 2. The adjustable base at the waist segment.

B. Hip Segment

The hip segment, mainly comprised of a passive actuator and a hinge, connects with the other two segments with carbon fiber struts. The hinge makes it possible for the thigh to rotate in the coronal plane, which is significant for the comfortability design since the additional degree of freedom extends the exoskeleton's working space from a 2-dimensional plane to a 3-dimensional space.

The passive actuator at the hip segment is shown in Fig. 3. Connectors 1 & 2, able to rotate around a pulley axle that connects them together, are bolted to the two carbon fiber struts, respectively. A torsional spring is sleeved on the axle with two bearings installed on its both ends. The pulley axle is kept in place by external retaining rings. The structural parameters of the torsional spring are listed in Table I.

The passive actuator can help assist hip flexion and extension during walking by periodically storing and releasing energy. When walking with the device, connector 1 remains relatively still with the waist while connector 2 rotates periodically with the movement of the thigh. That means the torsional spring should be compressed and thus stores the elastic potential energy when the hip extends backward, and release the energy thereafter in hip flexion until the torsional spring is completely restored to its normal state. This can be explained from the perspective of human physiology: the gluteus maximus, hamstring, and iliopsoas need to collaborate to generate hip flexion moment to decelerate the lower limb during the terminal stance and accelerate at pre-swing and initial swing phase of walking [14]. The passive actuator we designed utilizes the energy storage and release characteristic of the torsional spring to substitute part of the muscle work. Furthermore, the magnitude of the spring force and the time of its appearance can be finely adjusted by simply replacing the stopper with a different size. The working procedure can be divided into two stages in detail:

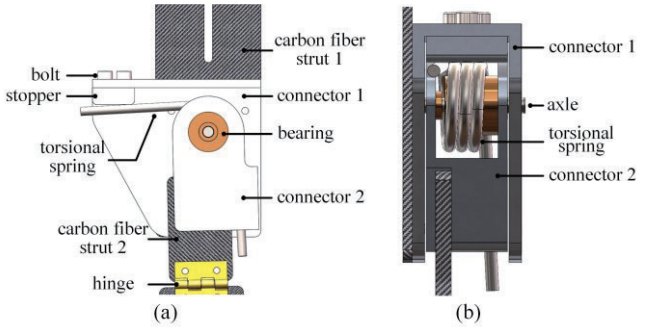

Fig. 3. The passive actuator at the hip segment. (a) Side view of the cross-section. (b) Rearview.

Step 1: The hip joint starts to extend back during the terminal stance phase when the torsion spring stores the energy and generates resisting torque. The resisting torque forces the person's hip joint to decelerate.

Step 2: After the hip joint extends to its maximum, the actuator releases the potential energy stored in *Step 1* and generates flexion torque in place of the iliopsoas. During this time, the actuator assists the hip joint to accelerate forward.

TABLE I.
VALUE OF PARAMETERS OF THE TORSIONAL SPRING

Structural Parameters	Value
Screw Pitch Diameter (mm)	26
Diameter (mm)	4
Circles	3
Swing Angle (°)	90
Length of the Fixed Arm (mm)	60
Length of the Swing Arm (mm)	60

C. Thigh Segment

Fitted with a misalignment compensation mechanism, the two carbon fiber thigh struts connect the hip segment with the thigh brace. An inertial sensor (JY61P, WitMotion, Shenzhen, China) is attached to the surface of the lower carbon fiber strut. A force sensor (HYLY-019, Hengyuan Sensing Technology, Bengbu, China), with a maximum load of 100 kg, is mounted at the back of the thigh brace to measure the assistive force generated by the motor. The force signal is then amplified by a weight transmitter (DY510, Bengbu Ocean Sensing System Engineering, Bengbu, China) and then transmitted to the real-time controller. The lower carbon fiber thigh strut is bolted with the thigh strap through stainless steel nuts and bolts.

The 3-dimensional assembly drawing and diagram of the misalignment compensation mechanism are shown in Fig. 4(a) and Fig. 4(b), respectively. It is clear that because of the unavoidable misalignment between the rotation axis of the hinge and that of the biological hip joint, the distance between the hinge and the thigh strap is constantly changing with hip abduction and adduction during walking, which means the abduction length does not correspond to the normal standing length shown in Fig. 4(b). In this case, undesired interaction force would occur if the length of the thigh strut is constant.

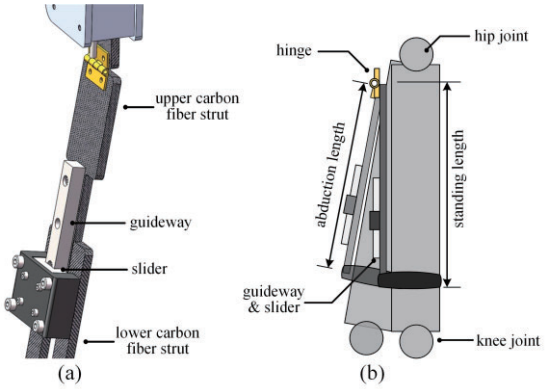

Fig. 4. The misalignment compensation mechanism. (a) SOLIDWORKS drawing. (b) Diagram of the mechanism.

This will cause discomfort to the user while walking and may also be dangerous. Utilizing a guideway-slider assembly to connect the upper and lower thigh strut components, which is proved to be effective for length adjustment with no resistance force, the misalignment compensation mechanism we designed can perfectly resolve the issue and thus improve the user's comfortability during walking.

III. CONTROL SCHEME

We proposed a hierarchical adaptive control framework for the hip exoskeleton. The high-level controller, sending the motor speed command to the low-level controller based on sensory information and user instruction, can switch between the *FOLLOW* mode (i.e., the person drives the exoskeleton with mere force while walking) and the *ASSIST* mode (i.e., the exoskeleton applies assistive force to the person at the proper time actively while walking) by the user's interaction with the exoskeleton. The low-level controller receives the speed command and calculates the desired current that is then transmitted to the motor.

A. System Framework

Fig. 5 shows the framework of the human-exoskeleton control system, which utilizes the two-level hierarchical controller to generate assistive force. The high-level controller is responsible for the desired motor angular velocity based on the user's command and the real-time sensor data, including the applied force derived from the force sensor, the angle and angular velocity of the thigh derived from the inertial sensor, the angle and angular velocity derived from the built-in encoder in the motor, and the current of the motor from the built-in current sensor in the motor. The motor current command is then calculated by a low-level controller and drives the motor to generate assistive force. The control frequency of the system is 200 Hz.

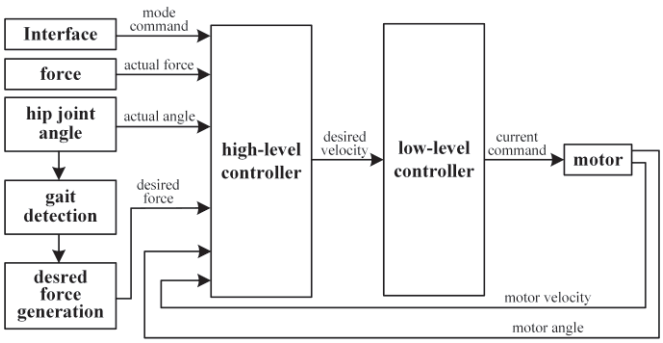

Fig. 5. Framework of the human-exoskeleton control system.

B. High-level Controller

We designed two working modes for the high-level controller: *FOLLOW* mode and *ASSIST* mode. In *FOLLOW* mode, the exoskeleton is almost "transparent" to the user, which means the interaction force of the human-exoskeleton system can be ignored. In this case, the relationship between the desired motor angle and the actual angle of the hip joint can be simplified as

$$\theta_{md} = k\theta_h, \quad (1)$$

where θ_{md} is the desired motor angle, θ_h is the hip joint angle, and k is a constant. The desired motor angular velocity in *FOLLOW* mode is determined by

$$\omega_{md} = k_p\left(\theta_{md} - \theta_m\right) + k_v k\omega_h, \tag{2}$$

where ω_{md} is the actual motor angular velocity, θ_m is the actual motor angle, ω_h is the hip joint angular velocity, k_p and k_v are the position error gain and the velocity error gain, respectively.

In *ASSIST* mode, the exoskeleton is expected to apply assistive force according to the desired force profile, and be "transparent" again when no force is needed to keep the cable slightly taut, which is particularly significant for the exoskeleton to provide safe, fast, and precise assistance in the next gait cycle. The desired motor angular velocity can be determined by

$$\omega_{md} = \begin{cases} k_f\left(F_d - F\right) - k_d\omega_m, & F_d > 0 \\ k_p\left(\theta_{md} - \theta_m\right) + k_v k\omega_h, & F_d = 0 \end{cases}, \tag{3}$$

where F_d is the desired assistive force and F is the actual force measured by the force sensor. k_p and k_d are the force error gain and the damping ratio gain, respectively.

C. Low-level Controller

The diagram of the dual closed-loop cascade PD controller, as a low-level controller, is shown in Fig. 6. The outer loop of the controller utilizes the error between the desired and actual angular velocity, ω_{md} and ω_m, to generate the desired current signal I_{md}. The signal, together with the actual current I_m, is transmitted into the inner loop of the controller that calculates the final current command I_c. The whole controller can be specified as below:

Outer loop:

$$i_{md} = k_{\omega\mathrm{P}}\left(\omega_{md} - \omega_m\right) + k_{\omega\mathrm{D}}\left(\dot{} \right. \tag{3}$$

Inner loop:

$$i_c = k_{i\mathrm{P}}\left(i_{md} - i_m\right) + k_{i\mathrm{D}}\left(\dot{} \right. \tag{4}$$

Here $k_{\omega\mathrm{P}}$ and $k_{\omega\mathrm{D}}$ are the proportional and derivative gain of the motor angular velocity error, respectively; $k_{i\mathrm{P}}$ and $k_{i\mathrm{D}}$ are the proportional and derivative gain of the motor current error, respectively.

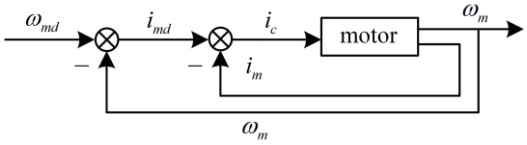

Fig. 6. Diagram of the low-level controller.

D. Assistive Force Profile

The assistive force profile is defined as a single-peak curve according to human walking biomechanics. The curve is realized by using two cubic splines joined at their peaks, which is similar to Zhang et al [15]. As shown in Fig. 7, we used four parameters to describe the curve: start time t_s, peak time t_p, end time t_e, and peak force F_p. The first three temporal-related parameters are normalized to percent stride and are denoted as X% (i.e., the time since the last heel strike divided by the average stride time [14]). Peak force refers to the maximum force that the exoskeleton will provide during walking.

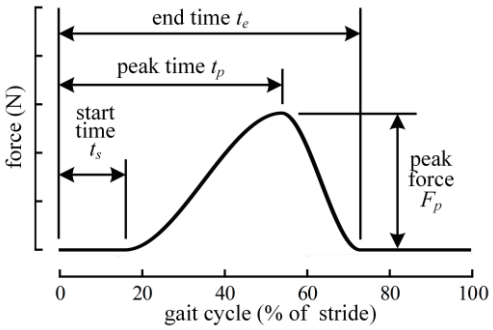

Fig. 7. Assistive force profile.

IV. Experiments and Results

To evaluate the effect of the exoskeleton on the wearer's gait kinematics and dynamics, and to determine the force and power delivered to the human, treadmill gait trials were performed on one healthy subject with no gait abnormalities. The author performed the experiments for this study, so no informed consent was required. The subject's age was 21, height was 180.1 cm and weight was 69.4 kg.

A. Experimental Platform Configuration

Fig. 8 shows the illustration of the experiment platform. The subject walked on a Bertec FIT instrumented split-belt treadmill (Bertec Corporation, Columbus, OH, USA) at a speed of 1.25 m/s. The force sensor mounted at the back of the thigh brace measured the assistive force generated by the exoskeleton. An inertial measurement unit fixed on the right side of the thigh brace measured the hip joint angle. All sensor data were then together transmitted to a real-time controller (DS1202, dSPACE, Paderborn, GmbH) that was connected to a PC for data processing, user-exoskeleton interaction and real-time control. As shown in Table II, the parameters of the control system were systematically adjusted to minimize the tracking error in both modes; the four parameters for the assistive force profile are manually optimized based on preliminary experiments, the values of which turned out to be very close to that in Collins et al. [16] and Walsh et al [12].

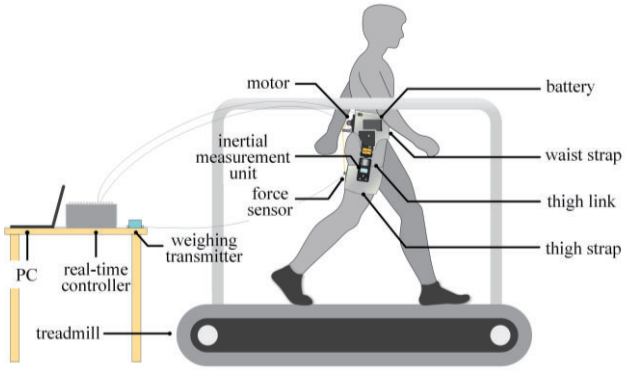

Fig. 8. Illustration of the experiment platform.

TABLE II.
VALUE OF PARAMETERS OF THE CONTROL SCHEME

High-Level Controller	k_p	k_v	k_f	k_d
	30	0.5	1	0.1
Low-Level Controller	$k_{\omega P}$	$k_{\omega D}$	k_{iP}	k_{iD}
	2.4	2.7	2	0
Assistive Force Profile	t_s (s)	t_p (s)	t_e (s)	F_p (N)
	85	5	25	30

B. *FOLLOW Mode Experiment*

The ideal performance of the exoskeleton in the *FOLLOW* mode is that the interaction force between humans and the exoskeleton is zero, which means the exoskeleton can completely follow the motion of the person. In addition, the flexible cable is required to keep slightly taut for safety concerns. Based on these considerations, two criteria for evaluating the exoskeleton's performance are summarized: the absolute interaction force and the tracking accuracy of the motor with respect to the hip joint angle.

The duration of the experiment is 120 seconds, and the middle 60 seconds were taken as the steady walking state for subsequent analysis. The subject reported nearly no resistance and discomfort during the experiment. The human-exoskeleton interaction force is shown in Fig. 9(a), and the comparison between the motor angle and the hip joint angle is shown in Fig. 9(b), both have been interpolated and normalized concerning the gait cycle of each stride. The solid curve in the plot is the average value, while the lower and the upper boundary indicates the standard deviation. Rigorously meticulous preparations were carried out before the official experiment begins to ensure the safety of the subject and the devices. It is worth noting that the walking state of the leg is detected according to the inertial sensor that measures the angle of the hip joint in real-time, so no extra sensors or pre-tests were required. See Fig. 9(a), the peak value of the average interaction force is 3.84 N mainly occurring at the initial swing phase of the gait cycle, which basically cannot be sensed by the subject. From Fig. 9(b) we can see that the measured motor angle tracked perfectly to the hip joint angle, with an average delay of 4.9% of the gait cycle, which is merely 35~45 milliseconds.

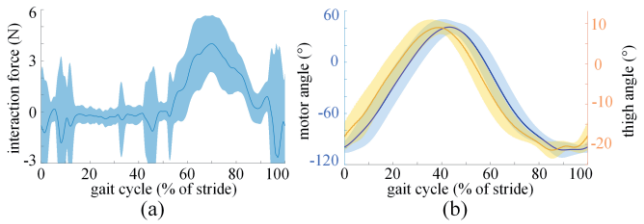

Fig. 9. Interaction force and angle tracking in *FOLLOW* mode. (a) Interaction force. (a) The angle of the motor and the hip joint.

C. *ASSIST Mode Experiment*

In the *ASSIST* mode, the exoskeleton is expected to provide assistive force as close to the desired force curve as possible and keeps following the subject's thigh when no force is needed to prepare for the next assistance. The experiment setup stayed the same as that in the *FOLLOW* mode.

Fig. 10(a) shows the force tracking performance. From Fig. 10(a), compared to the desired force, the measured assistive force had approximately an 8% lag at the start of assistance, but it tracked up quickly, ending up with a 1.8% lag and 2.3% overshoot at the peak. Fig. 10(b) shows the mechanical power applied by the exoskeleton, normalized to a gait cycle. Major assistive work can be seen at the terminal swing and loading response phase (95%~5%) of the gait cycle. The exoskeleton applied an average of 4.049 J assistive work per step through calculation. According to van Dijk et al, the average energy consumption per step of a 70 kg adult normal walking is about 23-28 J [17]. Thus, the exoskeleton can provide at least about 14% of the energy supply per step on average under the experimental scenario.

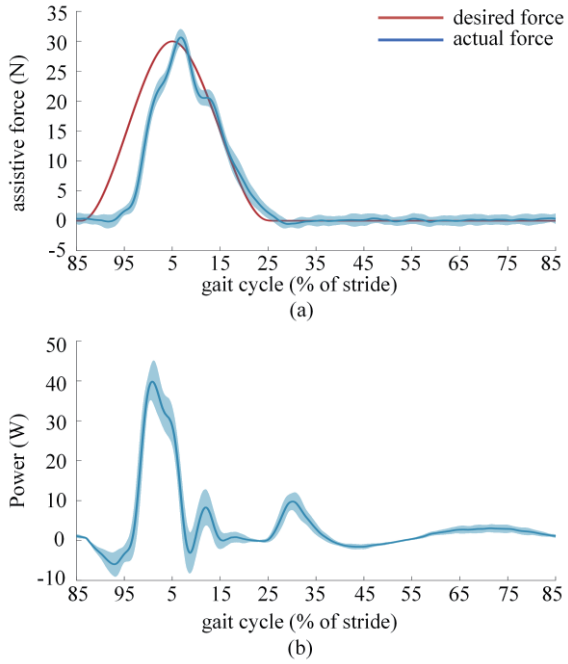

Fig. 10. Force tracking and applied power in *ASSIST* mode. (a) Desired and measured assistive force. (b) Assistive power provided by the exoskeleton.

V. DISCUSSION

The purpose of this research is to explore the design and control of a lightweight cable-driven hip exoskeleton for hip flexion-extension assistance with fast response and high tracking performance. From a hardware perspective, we modified the existing assistive hip exoskeleton by designing an additional degree of freedom at the coronal plane with a simple but useful component, a hinge. To avoid the misalignment problem of the rotation axis of the hinge and human hip joint, we presented an effective solution by adding a compensation mechanism at the thigh segment of the exoskeleton so that the length of the thigh was adjustable with no resistance during the process of hip abduction and adduction. Meanwhile, the utilization of the flexible cable and the torsional spring increased the compliance of the exoskeleton, showing a soft-rigid hybrid characteristic. One of our future studies aims at optimizing the mechanical design to be capable of integrating the flexible joint with variable stiffness and providing more effective torque for assistance. Besides, the next-generation exoskeleton should be a fully portable one,

which means all components including the controller and the processor should be on-board.

The exoskeleton can be "transparent" in *FOLLOW* mode and provide assistive force in *ASSIST* mode. Experimental results indicated the high precision of the controller and its effectiveness in providing assistive work during walking. Note that the control method here may be simplistic for preliminary verification and evaluation of the exoskeleton, and more advanced ones such as Computed Torque Control (CTC) [18], PD-LRN Control [15], Admittance/Impedance Control [19], may be utilized for the exoskeleton in complex scenarios with various tasks to demonstrate the practical applicability of hip exoskeletons. We also find that the resulting assistive power of the exoskeleton is in accordance with the joint power of the human hip measured by other scholars, where a peak power of 0.9 W/kg was reported at the loading response phase of the gait cycle [14]. This indicates that the designed exoskeleton has the potential of energy saving by replacing part of the hip work.

Analysis of various human physiological signals in the process of assistance will be applied in the future. When the exoskeleton generates forces on the human body, the activity of the corresponding muscles of the human leg will change. How the existing cable layout scheme will affect the comfort of the coxal muscle at large cable tension remains unclear temporarily. Additionally, many studies have shown that the surface electromyography (sEMG) signal and the subject's metabolic energy are essential indicators reflecting the effect of the exoskeleton assistance [20-22]. In the future, the sEMG signal and the metabolic energy consumption can be utilized for evaluating the effect of exoskeleton assistance, exploring the impact of different assistance modes, and optimizing the system parameter configurations to enhance the performance of the exoskeleton.

VI. Conclusion

In this paper, we designed a cable-driven hip exoskeleton that concentrates on lightweight, comfortability and human-machine interaction. The exoskeleton allows the hip to move in four directions: flexion, extension, abduction, and adduction. The motor, located at the back of the waist segment of the exoskeleton, provides assistive force through cable at terminal swing and early stance (85%~100%, 0~20%) of the gait cycle, while the passive actuator at the hip segment supplies hip flexion moment during the terminal stance, pre-swing and initial swing phase (30%~60%) of the gait cycle. For the control scheme, we proposed a hierarchical controller that determined the current command of the motor based on sensory information and user instruction. Experiments validated the effectiveness and comfortability of the exoskeleton. In the future, we will optimize the mechanical structure and control framework to enhance the performance of the exoskeleton. More human physiology signals, like sEMG and metabolic energy, will be involved to guide the mechanical and control designs to improve the interactions between the exoskeleton and users.

References

[1] A. T. Asbeck, K. Schmidt and C. J. Walsh, "Soft exosuit for hip assistance," *Robotics and Autonomous Systems*, vol. 73, pp. 101-110, 2015.

[2] A. Chu, H. Kazerooni and A. Zoss, "On the biomimetic design of the berkeley lower extremity exoskeleton (BLEEX)," in *Proceedings of the 2005 IEEE International Conference on Robotics and Automation*. IEEE, 2005, pp. 4345-4352.

[3] H. Kazerooni, J. L. Racine, L. Huang and R.Steger, "On the control of the berkeley lower extremity exoskeleton (BLEEX)," in *Proceedings of the 2005 IEEE International Conference on Robotics and Automation*. IEEE, 2005, pp. 4353-4360.

[4] ARGO Medical Technology, Ltd. [Online]. Available: http://rewalk.com/rewalk-personal-3.

[5] Ekso Bionics. [Online]. Available: http://eksobionics.com.

[6] Cyberdyne. [Online]. Available: https://www.cyberdyne.jp/english/products/HAL.

[7] Indego. [Online]. Available: https://www.indego.com.

[8] B. R. Umberger and J. Rubenson, "Understanding muscle energetics in locomotion: new modeling and experimental approaches,". *Exercise and Sport Sciences Reviews*, vol. 39, no. 2, pp. 59-67, 2011.

[9] K. Yasuhara, K. Shimada, T. Koyama, T. Ido, K. Kikuchi and Y. Endo, "Walking assist device with stride management system," *Honda R&D Technical Review*, vol. 21, no. 2, pp. 54-63, 2009.

[10] T. Zhang, M. Tran and H. H. Huang, "NREL-Exo: A 4-DoFs wearable hip exoskeleton for walking and balance assistance in locomotion," in *2017 IEEE/RSJ International Conference on Intelligent Robots and Systems (IROS)*. IEEE, 2017, pp. 508-513.

[11] F. Giovacchini, F. Vannetti, M. Fantozzi, M. Cempini, M. Cortese, A. Parri, T. Yan, D, Lefeber and N. Vitiello, "A light-weight active orthosis for hip movement assistance," *Robotics and Autonomous Systems*, vol. 73, pp. 123-134, 2015.

[12] A. T. Asbeck, K. Schmidt and C. J. Walsh, "Soft exosuit for hip assistance," *Robotics and Autonomous Systems*, vol. 73, pp. 102-110, 2015.

[13] V. L. Chiu, M. Raitor and S. H. Collins, "Design of a hip exoskeleton with actuation in frontal and sagittal planes,". *IEEE Transactions on Medical Robotics and Bionics*, vol. 3, no. 3, pp. 773-782, 2021.

[14] M. W. Whittle, "Gait analysis: an introduction," Butterworth-Heinemann, 2014.

[15] W. Wang, J. Chen, Y. Ji, W. Jin, J. Liu and J. Zhang, "Evaluation of lower leg muscle activities during human walking assisted by an ankle exoskeleton," *IEEE Transactions on Industrial Informatics*, vol. 16, no. 11, pp. 7168-7176, 2020.

[16] G. M. Bryan, P. W. Franks, S. C. Klein, R. J. Peuchen and S. H. Collins, "A hip–knee–ankle exoskeleton emulator for studying gait assistance," *The International Journal of Robotics Research*, vol. 40, no. 4-5, pp. 722-746, 2021.

[17] W. van Dijk and H. Van der Kooij, "XPED2: A passive exoskeleton with artificial tendons," *IEEE Robotics & Automation Magazine*, vol. 21, no. 4, pp. 56-61, 2014.

[18] R. H. Middletone and G. C. Goodwin, "Adaptive computed torque control for rigid link manipulators," in *1986 25th IEEE Conference on Decision and Control*. IEEE, 1986, pp. 68-73.

[19] T. Zhang, M. Tran and H. Huang, "Design and experimental verification of hip exoskeleton with balance capacities for walking assistance," *IEEE/ASME Transactions on Mechatronics*, vol. 23, no. 1, pp. 274-285, 2018.

[20] F. A. Panizzolo, E. Annese, A. Paoli and G. Marcolin, "A single assistive profile applied by a passive hip flexion device can reduce the energy cost of walking in older adults," *Applied Sciences*, vol. 11, no. 6, pp. 2851, 2021.

[21] K. Gui, H. Liu, and D. Zhang, "A practical and adaptive method to achieve EMG-based torque estimation for a robotic exoskeleton," *IEEE/ASME Transactions on Mechatronics*, vol. 24, no. 2, pp. 483-494, 2019.

[22] J. Kim, G. Lee, R. Heimgartner, D. A. Revi, N. Karavas, D. Nathanson, I. Galiana, A. Eckert-Erdheim, P. Murphy, D. Perry, N. Menard, D. K. Choe, P. Malcom and C. J. Walsh, "Reducing the metabolic rate of walking and running with a versatile, portable exosuit," *Science*, vol. 365, no. 6454, pp. 668-672, 2019.